



North Atlantic Oscillation controls on oxygen and hydrogen isotope gradients in winter precipitation across Europe; implications for palaeoclimate studies

Michael Deininger¹, Martin Werner², and Frank McDermott^{1,3}

¹UCD School of Earth Sciences, University College Dublin, Belfield, Dublin 4, Ireland

²Alfred Wegener Institute, Helmholtz Centre for Polar and Marine Research, Bussestraße 24, 27570 Bremerhaven, Germany

³UCD Earth Institute, University College Dublin, Belfield, Dublin 4, Ireland

Correspondence to: Michael Deininger (michael.deininger@ucd.ie)

Received: 7 July 2016 – Published in Clim. Past Discuss.: 14 July 2016

Accepted: 24 October 2016 – Published: 28 November 2016

Abstract. Winter (October to March) precipitation $\delta^{18}\text{O}_\text{p}$ and δD_p values in central Europe correlate with the winter North Atlantic Oscillation index (wNAOi), but the causal mechanisms remain poorly understood. Here we analyse the relationships between precipitation-weighted $\delta^{18}\text{O}_\text{p}$ and δD_p datasets ($\delta^{18}\text{O}_{\text{pw}}$ and $\delta\text{D}_{\text{pw}}$) from European GNIP and ANIP stations and the wNAOi, with a focus on isotope gradients. We demonstrate that longitudinal $\delta^{18}\text{O}_{\text{pw}}$ and $\delta\text{D}_{\text{pw}}$ gradients across Europe (“continental effect”) depend on the wNAOi state, with steeper gradients associated with more negative wNAOi states. Changing gradients reflect a combination of air temperature and variable amounts of precipitable water as a function of the wNAOi. The relationships between the wNAOi, $\delta^{18}\text{O}_{\text{pw}}$ and $\delta\text{D}_{\text{pw}}$ can provide additional information from palaeoclimate archives such as European speleothems that primarily record winter $\delta^{18}\text{O}_{\text{pw}}$. Comparisons between present-day and past European longitudinal $\delta^{18}\text{O}$ gradients inferred from Holocene speleothems suggest that atmospheric pressure configurations akin to negative wNAO modes dominated the early Holocene, whereas patterns resembling positive wNAO modes were more common in the late Holocene, possibly caused by persistent shifts in the relative locations of the Azores High and the Icelandic Low.

1 Introduction

Stable oxygen and hydrogen isotopes ($\delta^{18}\text{O}$, δD ; relative to Vienna Standard Mean Ocean Water) in precipitation have been analysed extensively since the 1950s (Dansgaard, 1954; Craig, 1961; Craig and Gordon, 1965) to decipher environmental processes that control their variations and to facilitate their use in palaeoclimatology (Dansgaard, 1964; Gat, 1996; Rozanski et al., 1992; Aggarwal et al., 2012). The Global Network of Isotopes in Precipitation (GNIP) program initiated in 1958 by the International Atomic Energy Agency (IAEA) and the World Meteorological Organization (WMO) has operated since 1961 and has made great progress towards these aims (e.g. Dansgaard, 1964; Rozanski et al., 1992). For the European sector of the GNIP program, 438 stations have operated, with the oldest records from the GNIP stations at Valencia Observatory in Ireland (since 1958) and at Hohe Warte (Vienna, Austria) since 1960. The processes that drive $\delta^{18}\text{O}$ values in precipitation ($\delta^{18}\text{O}_\text{p}$) at these stations have been discussed extensively in the literature, focusing mainly on air temperature, altitude and the “continental effect” (Rozanski et al., 1982; Stumpp et al., 2014; Schürch et al., 2003; Lykoudis and Argiriou, 2011; Fischer and Baldini, 2011). In recent years, several studies have investigated the relationship between the North Atlantic Oscillation (NAO) – the major atmospheric mode of European winter climate, (Hurrell et al., 2003; Hurrell and VanLoon, 1997; Hurrell, 1995) – and $\delta^{18}\text{O}_\text{p}$ at specific stations (Baldini et al., 2008; Langebroek et al., 2011; Field, 2010). More recently, the ef-

fect of the east Atlantic pattern, the second major mode of atmospheric pressure variability in the North Atlantic region (Barnston and Livezey, 1987) on the relationship between the winter NAO index (wNAOi) and the $\delta^{18}\text{O}_\text{P}$ in Europe has been examined (Comas-Bru et al., 2016). A complementary approach, developed here, is to document and seek to understand the longitudinal gradients in winter rainfall $\delta^{18}\text{O}_\text{P}$ across Europe and to link these to different states of the NAO.

Here we present a detailed station-based evaluation of the effects of the wNAOi on precipitation-weighted $\delta^{18}\text{O}_\text{P}$ and δD_P values ($\delta^{18}\text{O}_\text{pw}$ and δD_pw) during the winter season for continental Europe and the Alps. We demonstrate that the well-documented longitudinal gradient in $\delta^{18}\text{O}_\text{pw}$ and δD_pw across the European continent (often referred to as the continental effect) depends on the state of the winter NAO index (wNAOi), through a combination of air temperature and atmospheric precipitation history effects. The downstream effects of this wNAOi-linked variability can also be detected in the $\delta^{18}\text{O}_\text{pw}$ and δD_pw values at stations north of the Alpine divide. We also make use of the $\delta^{18}\text{O}_\text{pw}$ and δD_pw outputs from an isotope-enabled general circulation model ECHAM5-wiso (Werner et al., 2011; Langebroek et al., 2011) to better evaluate the NAO dependence of the longitudinal isotope gradients. This study improves our understanding of the significance of inferred past changes in $\delta^{18}\text{O}_\text{pw}$ or δD_pw gradients across Europe, for example during the course of the Holocene (e.g. McDermott et al., 2011) by linking modern $\delta^{18}\text{O}_\text{pw}$ and δD_pw gradients to different states of the wNAO and/or changes in the European continental temperature gradient and atmospheric precipitation histories.

2 Data and methods

2.1 Station-based data

Monthly winter (October to March) $\delta^{18}\text{O}_\text{P}$, δD_P , temperature and precipitation data from 37 European stations were used to investigate the dependence of $\delta^{18}\text{O}_\text{pw}$ and δD_pw values on the wNAOi (Fig. 1).

Thirty-one of these stations are part of the GNIP network and six are part of the Austrian Network of Isotopes in Precipitation (ANIP). The data from the ANIP stations originate from Humer (1995) and the ANIP home page (<http://wisa.bmlfuw.gv.at/daten.html>). The GNIP stations were selected based on recent findings, showing that the unweighted winter (December to March) $\delta^{18}\text{O}_\text{P}$ and δD_P values at these stations are significantly correlated with the wNAOi (Baldini et al., 2008). The ANIP stations were selected for their long records starting in the early 1970s and their location, which ensures that there are sufficient $\delta^{18}\text{O}_\text{P}$ and δD_P measurements in the Alps for the purposes of this study. For our analysis, the wNAOi is the average winter value calculated from the monthly PC (principle component)-based NAOi values from December to March (Hurrell, 1995) downloaded

from the Climate Data Guide.¹ For every station, the $\delta^{18}\text{O}_\text{pw}$ and δD_pw values were calculated for each winter, using the monthly $\delta^{18}\text{O}_\text{P}$ and δD_P values, weighted by the monthly precipitation amounts, for the period October to March (6 months) and December to February (3 months). The studied periods are chosen on the one hand because during December to February the NAO exerts its strongest influence on the European winter climate (e.g. Hurrell, 1995) and we expect to observe the strongest influence on $\delta^{18}\text{O}_\text{P}$ and δD_P in this 3-month period and on the other hand because the main infiltration period for precipitation in central Europe is from October to March and is, therefore, the period of interest for palaeoclimate archives recording the infiltrated $\delta^{18}\text{O}_\text{pw}$ and δD_pw in this 6-month interval (e.g. speleothems). For further analysis, the winter $\delta^{18}\text{O}_\text{pw}$ and δD_pw values (6 months and 3 months) of every station are grouped into six classes depending on the wNAOi. The wNAOi was subdivided into six classes (bins): (i) $1.6 \leq \text{wNAOi}$; (ii) $0.8 \leq \text{wNAOi} < 1.6$; (iii) $0 \leq \text{wNAOi} < 0.8$; (iv) $-0.8 \leq \text{wNAOi} < 0$; (v) $-1.6 \leq \text{wNAOi} < -0.8$; and (vi) $\text{wNAOi} < -1.6$. This results in six compilations of $\delta^{18}\text{O}_\text{pw}$ and δD_pw values for every station. For every station, the median of every compilation was calculated. An example is given in Fig. 2, which shows how the data were processed, resulting in six median $\delta^{18}\text{O}_\text{pw}$ and δD_pw values for the Garmisch-Partenkirchen station (no. 24 in Fig. 1).

For the analysis of the processed $\delta^{18}\text{O}_\text{pw}$ and δD_pw values, the stations were also subdivided into “continental” stations, which includes all stations with an altitude ≤ 350 m and no (or negligible) Mediterranean influence (distance to the Mediterranean coastline > 100 km; 13 stations), and stations with an altitude > 350 m. The latter stations were divided into two groups: continental stations with an altitude higher than 350 m (3 stations) and Alpine stations (17 stations). Furthermore, four Mediterranean GNIP stations south of the Alps were analysed to better validate the $\delta^{18}\text{O}_\text{pw}$ and δD_pw values of the Alpine regions (Fig. 1).

3 Results

3.1 Results of the longitudinal $\delta^{18}\text{O}_\text{pw}$ and δD_pw gradients (continental stations)

To study the relationship between the wNAOi classes and the longitudinal $\delta^{18}\text{O}_\text{pw}$ and δD_pw gradients during the winter season, $\delta^{18}\text{O}_\text{pw}$ and δD_pw datasets of a total of 13 continental GNIP stations are analysed. (This includes the two maritime sites: Valencia Observatory, Ireland (station no. 1), and Wallingford, England (station no. 2).) The most westerly station is at -10.25° E (Valencia Observatory; Ireland) and the easternmost station is at 19.85° E (Kraków, Poland;

¹The Climate Data Guide: Principal Component based North Atlantic Oscillation (NAO) Index: <https://climatedataguide.ucar.edu/climate-data/>.

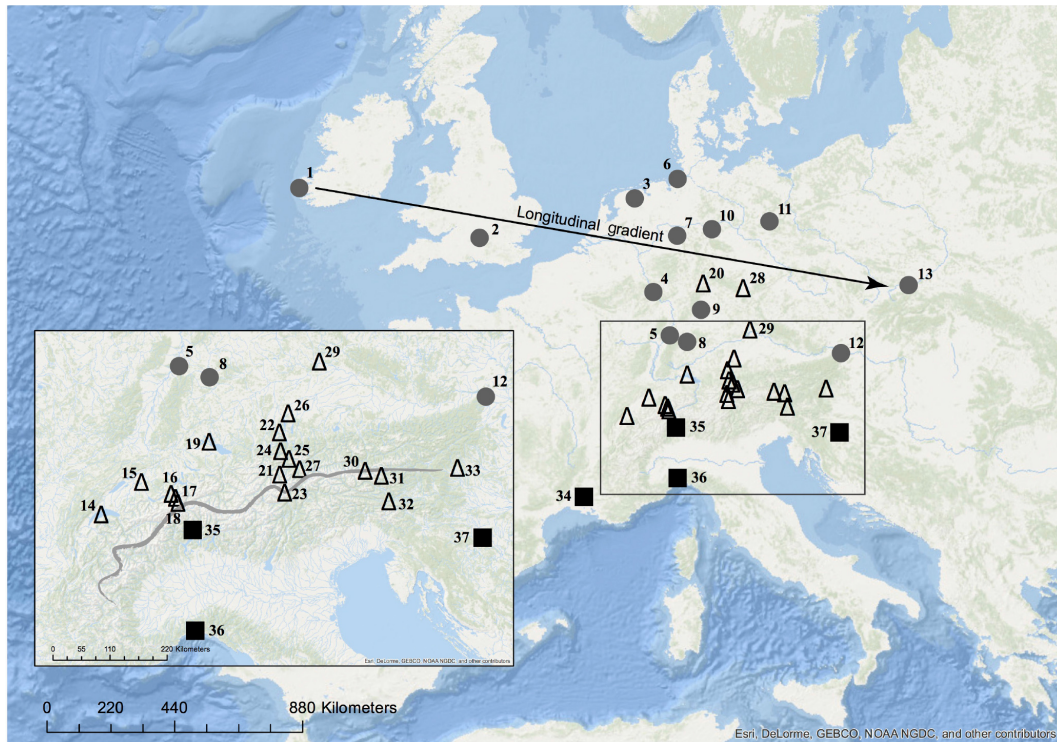


Figure 1. Map showing the location of all investigated stations: closed grey circles show the location of continental stations (altitude ≤ 350 m with no Mediterranean influence); open triangles indicate alpine and high-altitude (> 350 m) stations; closed squares show the location of “Mediterranean-influenced” stations. The grey line in the box indicates the Alpine divide. Station codes for continental stations (from west to east): (1) Valencia (Observatory); (2) Wallingford; (3) Groningen; (4) Koblenz; (5) Karlsruhe; (6) Cuxhaven; (7) Bad Salzuflen; (8) Stuttgart (Cannstatt); (9) Würzburg; (10) Braunschweig; (11) Berlin; (12) Vienna (Hohe Warte); (13) Kraków (Wola Justowska). For high-altitude stations: (14) Thonon-les-Bains; (15) Bern; (16) Meiringen; (17) Guttannen; (18) Grimsel; (19) Konstanz; (20) Wasserkuppe-Rhoen; (21) Längenfeld; (22) Hohenpeißenberg; (23) Obergurgl; (24) Garmisch-Partenkirchen; (25) Scharnitz; (26) Neuherrberg; (27) Patscherkofel; (28) Hof-Hohensaas; (29) Regensburg; (30) Bockstein; (31) St. Peter; (32) Villacher Alpe and (33) Graz University. For Mediterranean-influenced stations: (34) Avignon; (35) Locarno; (36) Genoa (Sestri) and (37) Zagreb.

Fig. 1). These continental stations show a positive sensitivity of $\delta^{18}\text{O}_{\text{pw}}$ and $\delta\text{D}_{\text{pw}}$ to the wNAOI (Fig. 3), i.e. a positive linear relationship with the wNAOI for the investigated continental station datasets, resulting in more positive median $\delta^{18}\text{O}_{\text{pw}}$ and $\delta\text{D}_{\text{pw}}$ values for higher wNAOI classes, as in Fig. 2 for Garmisch-Partenkirchen. An exception to this observation is the GNIP station Valencia Observatory (Station 1), where the $\delta^{18}\text{O}_{\text{pw}}$ and $\delta\text{D}_{\text{pw}}$ values do not show a clear linear relationship compared to the other continental stations for either the 3-month (Fig. 3a and c) or 6-month (Fig. 3b and d) winter periods. Similar behaviour is seen in the data for the Wallingford GNIP station (Station 2) for the 6-month winter period (Fig. 3b and d). This behaviour is likely to be caused by the proximity of these two maritime stations to the North Atlantic. It is notable that for most stations, the sensitivity of $\delta^{18}\text{O}_{\text{pw}}$ and $\delta\text{D}_{\text{pw}}$ to the wNAOI is higher for the 3-month winter period than for the 6-month winter period (Fig. 3). The median sensitivity for $\delta^{18}\text{O}_{\text{pw}}$ is 0.87 (3 month) and 0.57 (6 month) ‰/wNAOI unit, and for $\delta\text{D}_{\text{pw}}$, it is 6.87 (3 month) and 4.44 (6 month) ‰/wNAOI unit. This likely

reflects the fact that the mode of the wNAOI (December to March) exerts the strongest influence on European winter meteorology (e.g. Hurrell, 1995; Hurrell et al., 2003) and so also on $\delta^{18}\text{O}_{\text{pw}}$ and $\delta\text{D}_{\text{pw}}$ (see discussion in Sect. 4.1).

To investigate the dependence of the longitudinal $\delta^{18}\text{O}_{\text{pw}}$ and $\delta\text{D}_{\text{pw}}$ gradients from these 13 continental stations on the wNAOI classes, the gradient slopes were calculated for each of the six wNAOI classes. For all winter month periods the slope is negative (towards the east), indicating that the $\delta^{18}\text{O}_{\text{pw}}$ and $\delta\text{D}_{\text{pw}}$ values become more negative towards the east. Furthermore, the slopes of the longitudinal $\delta^{18}\text{O}_{\text{pw}}$ and $\delta\text{D}_{\text{pw}}$ gradients of the continental stations becomes steeper for winters with more negative wNAOI classes (Fig. 4). This means that ^{18}O and ^2H are more efficiently removed from the atmospheric moisture with distance from the western margin, resulting in more strongly negative $\delta^{18}\text{O}_{\text{pw}}$ and $\delta\text{D}_{\text{pw}}$ values along the longitudinal transect during more negative NAO winters compared with more positive NAO winters. Furthermore, the slope is steeper for the 3-month (DJF) averages compared with that for the 6-winter month averages.

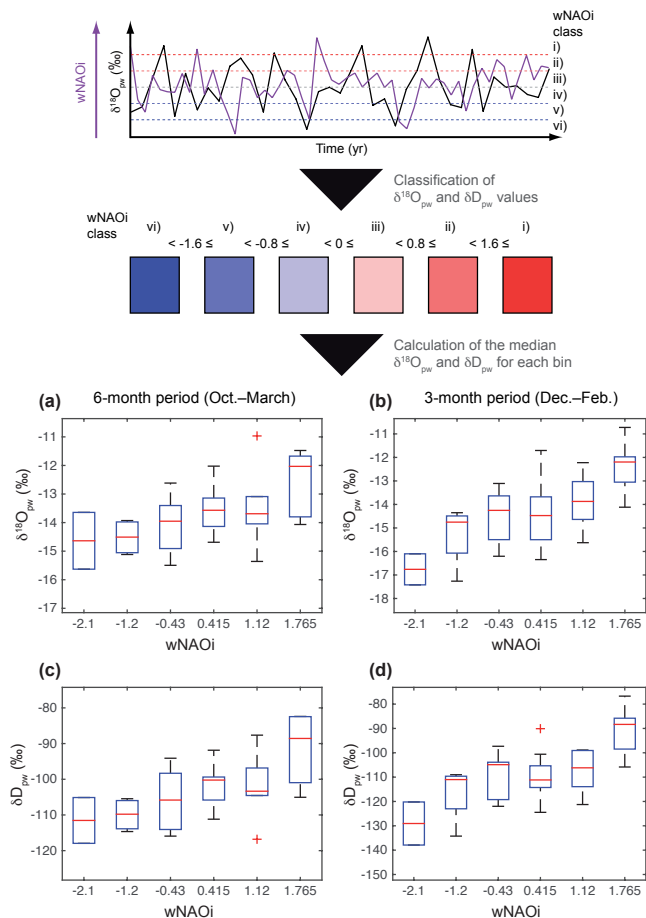


Figure 2. The upper part of the figure depicts how the precipitation-weighted $\delta^{18}\text{O}_{\text{pw}}$ and $\delta\text{D}_{\text{pw}}$ values are classified here into six classes depending on the wNAOI. Median values are calculated for every class, and this is used for further analysis. Panels (a) to (d) show the processed results for the six classes for one example of a GNIP station (Garmisch-Partenkirchen, Germany), for which $\delta^{18}\text{O}_{\text{pw}}$ and $\delta\text{D}_{\text{pw}}$ values have a typical sensitivity to wNAOI (see Fig. 3). The left panels show the box plots for the 6-month period (October to March) and the right panels for the 3-month period (December to February). The upper panels illustrate the $\delta^{18}\text{O}_{\text{pw}}$ values, the lower panels the $\delta\text{D}_{\text{pw}}$ values. Every box plot illustrates the statistical variables (median, min., max., and 25 and 75 % quantile) for every wNAOI class from lowest to highest (left to right). For the individual wNAOI classes, the red line illustrates the median of the data compilation; the edges of the blue rectangles mark the 25 and 75 % quantile; the black bars illustrates the minimum and maximum values, and the red cross denotes “outliers”.

Comparison of the longitudinal $\delta^{18}\text{O}_{\text{pw}}$ and $\delta\text{D}_{\text{pw}}$ gradients derived from ECHAM5-wiso simulations with those from the station-based data show that slopes from the ECHAM5-wiso data reproduce the observed station-based slopes quite well (Fig. 4). Only the slopes determined for the most negative wNAOI class of the 6-month winter period level off from the empirically determined slopes (Fig. 4a

and c). Overall, however, there is good agreement between the ECHAM5-wiso isotope gradients and those derived from the observational datasets (see the Supplement for a detailed discussion on ECHAM5-wiso simulations).

3.2 Alpine stations and other stations with an altitude > 350 m

Data from European stations with an altitude greater than 350 m are separated into two groups: Alpine stations and non-Alpine stations. The non-Alpine stations include Wasserkuppe-Rhoen (no. 20; 921 m), Hof-Hohensaas (no. 28; 567 m) and Regensburg (no. 29; 377 m), all located in Germany (Fig. 1). These show similar $\delta^{18}\text{O}_{\text{pw}}$ and $\delta\text{D}_{\text{pw}}$ sensitivity to the wNAOI as the other continental stations (Fig. 3). The Alpine stations include a total of 17 stations that are well distributed over the Alps (Fig. 1). These data allow an evaluation of precipitation $\delta^{18}\text{O}_{\text{pw}}$ and $\delta\text{D}_{\text{pw}}$ values and patterns in the entire Alpine region as a function of the wNAOI. The sensitivity analysis of $\delta^{18}\text{O}_{\text{pw}}$ and $\delta\text{D}_{\text{pw}}$ of the Alpine stations reveals a somewhat more complex relationship with the wNAOI. For the 3-month winter period, the $\delta^{18}\text{O}_{\text{pw}}$ data from the Thonon-les-Bains (14), Längenfeld (21), Obergurgl (23), Böckstein (30), St. Peter (31), Villacher Alpe (32) and Graz University (33) stations have a weak or absent relationship with the wNAOI, while the $\delta^{18}\text{O}_{\text{pw}}$ and $\delta\text{D}_{\text{pw}}$ data from the other Alpine stations have a similar sensitivity to the wNAOI as the continental stations (Fig. 3a). The $\delta\text{D}_{\text{pw}}$ data show similar results to $\delta^{18}\text{O}_{\text{pw}}$, but there are different results for some other stations. For Thonon-les-Bains (14) the relationship between $\delta\text{D}_{\text{pw}}$ and the wNAOI is stronger compared to $\delta^{18}\text{O}_{\text{pw}}$, whereas the relationship for Grimsel is weaker (18; Fig. 3c). For the 6-month winter period, the $\delta^{18}\text{O}_{\text{pw}}$ sensitivity to the wNAOI for most of the Alpine stations is comparably strong to that of the continental stations. Only the stations at Thonon-les-Bains (14), Längenfeld (21), Böckstein (30), St. Peter (31), Villacher Alpe (32) and Graz University (33) show a weak relationship with the wNAOI (like for the 3-month winter period). The Obergurgl station (23) has a stronger relationship with the wNAOI compared with the 3-month winter period but has a smaller average $\delta^{18}\text{O}_{\text{pw}}$ sensitivity compared with the other Alpine stations. The highest $\delta^{18}\text{O}_{\text{pw}}$ sensitivity can be found for Hohenpeißenberg (22) and Regensburg (29) and is 0.77‰/wNAOI unit (Fig. 3b). The $\delta\text{D}_{\text{pw}}$ sensitivity of the Alpine stations for the 6-month winter period shows a similar relationship as for the 3-month winter period. For stations in Bern (15), Guttannen (17), Obergurgl (23) and Villacher Alpe (32), however, the conclusion is different compared with the 3-month winter period. The relationship of $\delta\text{D}_{\text{pw}}$ to the wNAOI is weaker for Bern (17), whereas it is stronger for the other stations. The highest sensitivity is observed for the Thonon-les-Bains (14) and Meiringen (16) stations and is 7.42 and 8.84‰/wNAOI unit, respectively (Fig. 3d).

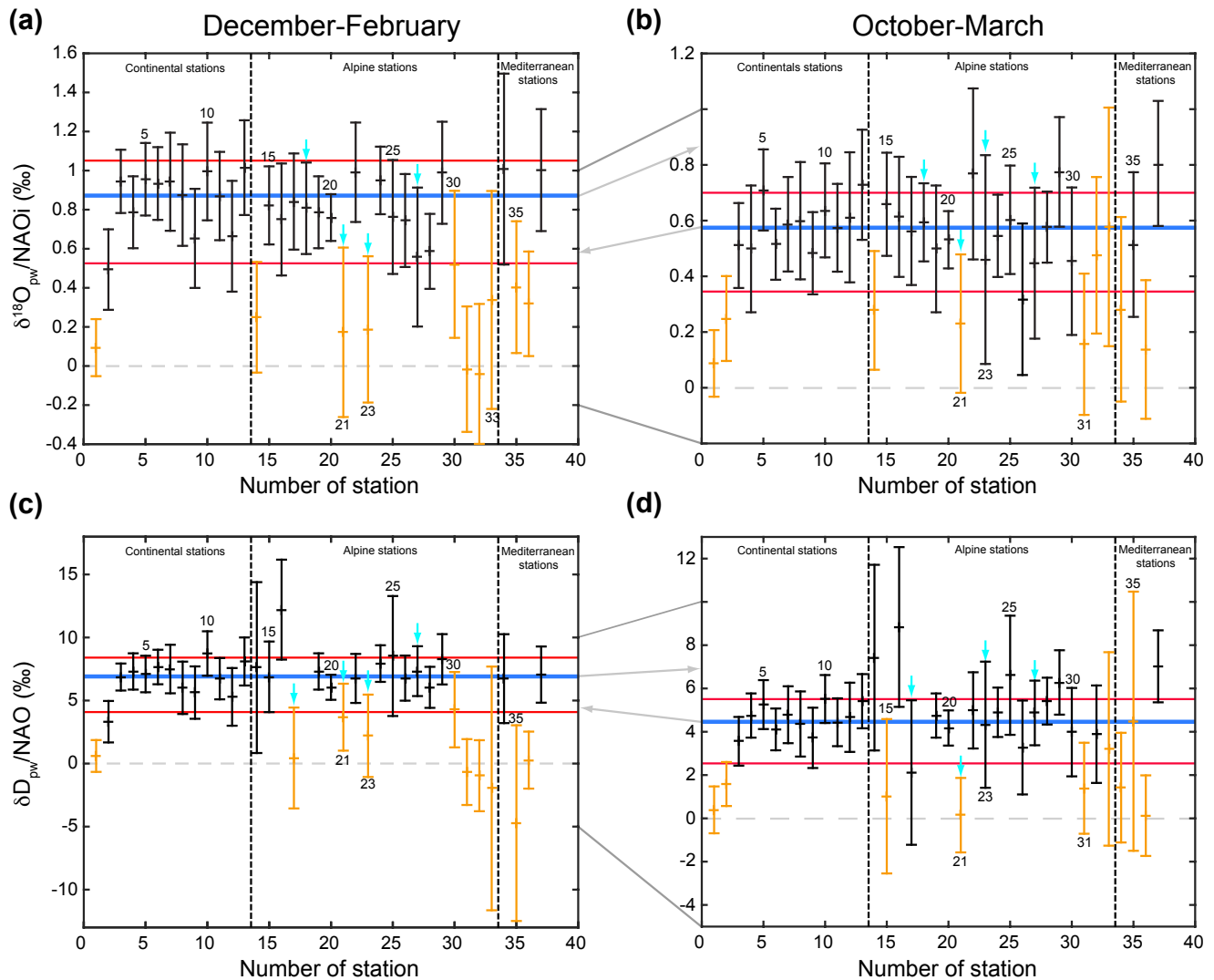


Figure 3. The panels illustrate the slopes of the linear regressions between yearly $\delta^{18}\text{O}_{\text{pw}}$ (**a, b**) and $\delta\text{D}_{\text{pw}}$ (**c, d**) and the wNAOI for each individual station for the 3-month winter period (December–February; left panels) and the 6-month winter period (October–March; right panels). If the slope is illustrated in black, the linear correlation coefficient is greater than 0.3; otherwise, it is shown in orange. The blue lines indicate the median values of all continental stations; the upper and lower red lines highlight the 1σ standard deviation around the mean value. The grey dashed lines indicate a slope of 0 (i.e. no sensitivity). Garmisch-Partenkirchen station (24), whose sensitivity on the wNAOI classes is shown in detail in Fig. 2, is typical of the investigated stations. The cyan-coloured arrows indicate stations closest to the Alpine divide. Numbers indicate station codes as in Fig. 1.

4 Discussion

4.1 Longitudinal $\delta^{18}\text{O}_{\text{pw}}$ and $\delta\text{D}_{\text{pw}}$ gradients

To explain the change in the slopes of the longitudinal winter $\delta^{18}\text{O}_{\text{pw}}$ and $\delta\text{D}_{\text{pw}}$ gradients (Fig. 4), the measured temperatures and the amount of precipitation at the GNIP stations are evaluated. The GNIP station based continental temperature and precipitation gradients for the different wNAOI classes show that the slopes of the longitudinal winter temperature gradients become steeper for lower wNAOI values and are always negative (i.e. average winter temperatures are always

lower in the east), but no equivalent relationship is observed for the slopes of the winter precipitation gradients (Fig. 5). (The following conclusions are not hampered if the two maritime sites Valencia Observatory (station no. 1) and Wallingford (station no. 2) (Fig. 1) are omitted from the compilation of all continental stations (Fig. S1 in the Supplement).) The temperature relationships suggest that while the winter air temperature clearly becomes colder from west to east, a higher average air temperature gradient between western and eastern Europe occurs in more negative wNAOI winters. Furthermore, the intercept of the linear regression is progressively smaller for more negative wNAOI modes, suggesting

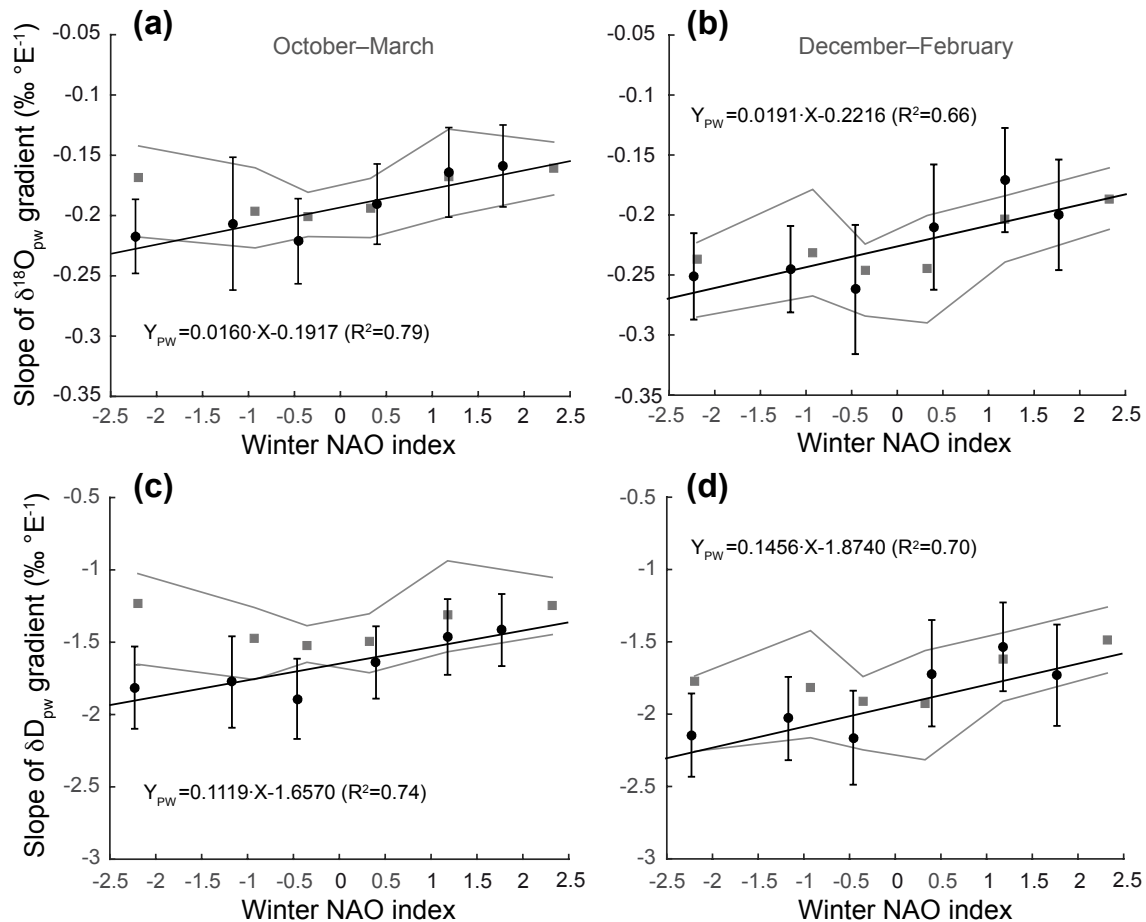


Figure 4. Illustration of the slopes of the $\delta^{18}\text{O}_{\text{pw}}$ (a, b) and $\delta\text{D}_{\text{pw}}$ (c, d) longitudinal gradients across Europe (filled circles) – and their respective standard errors – calculated from 13 continental GNIP stations for the 6-month (October–March; a and c) and 3-month (December to February; b and d) winter period. More negative wNAOi classes result in a steeper isotope gradient across Europe in winter and, therefore, more strongly depleted $\delta^{18}\text{O}_{\text{pw}}$ and $\delta\text{D}_{\text{pw}}$ values with increasing distance (towards the east) from the European western margin. The coefficient for the linear regression between the observed slopes and the class of the wNAOi is 0.016 ± 0.004 ($r^2 = 0.79$; $p < 0.05$) for Fig. 1a, 0.019 ± 0.006 ($r^2 = 0.65$; $p = 0.0502$) for Fig. 1b, 0.111 ± 0.033 ($r^2 = 0.74$, $p < 0.05$) for Fig. 1c and 0.146 ± 0.048 ($r^2 = 0.70$, $p < 0.05$) for Fig. 1d (units are $\text{‰} \cdot \text{E}^{-1} / \text{wNAOi}$). These equations state the results from the linear regression where Y_{pw} is the slope of the $\delta^{18}\text{O}_{\text{pw}}$ or $\delta\text{D}_{\text{pw}}$ gradient and X is the wNAOi. The filled grey squares show the median slopes of the ECHAM5-wiso simulations; the grey envelope indicates the 25 and 75 % quantiles of the ECHAM5-wiso slopes.

general cooler conditions in central Europe during negative wNAOi modes. This is consistent with the general relationship between the wNAOi and winter air temperatures for central Europe (e.g. Hurrell, 1995; Comas-Bru and McDermott, 2013). Curiously, for the most negative wNAOi class, the slope of the temperature gradient does not follow the general trend and has a lower value, comparable to more positive winter wNAOi modes, suggesting a smaller temperature difference between western and eastern Europe under these conditions. The reason for this change is unclear and possibly reflects a relationship between the cyclone variability and the NAO (Gulev et al., 2001), which may increase the frequency of incursions of cold easterly winds into western Europe during very negative wNAO modes.

The observed temperature slopes can be used to calculate the expected air-temperature-driven difference in $\delta^{18}\text{O}_{\text{pw}}$ and $\delta\text{D}_{\text{pw}}$ between the western- and easternmost GNIP stations using theoretical temperature sensitivities for $\delta^{18}\text{O}_{\text{P}}$ and $\delta\text{D}_{\text{P}}$ (e.g. from Dansgaard, 1964). The theoretical changes in $\delta^{18}\text{O}_{\text{pw}}$ and $\delta\text{D}_{\text{pw}}$ between the western- and easternmost GNIP stations (the longitudinal difference between the Valencia (Observatory) and Kraków (Wola Justowska) is 30.1°) were calculated as follows. First, the temperature difference between these two stations was calculated from the temperature slope for the different wNAOi classes. For example, for the highest wNAOi class, the slope of the observed temperature gradient is -0.19 and $-0.26 \text{ K} \cdot \text{E}^{-1}$ for the 6-month and 3-month winter period, resulting in a temperature dif-

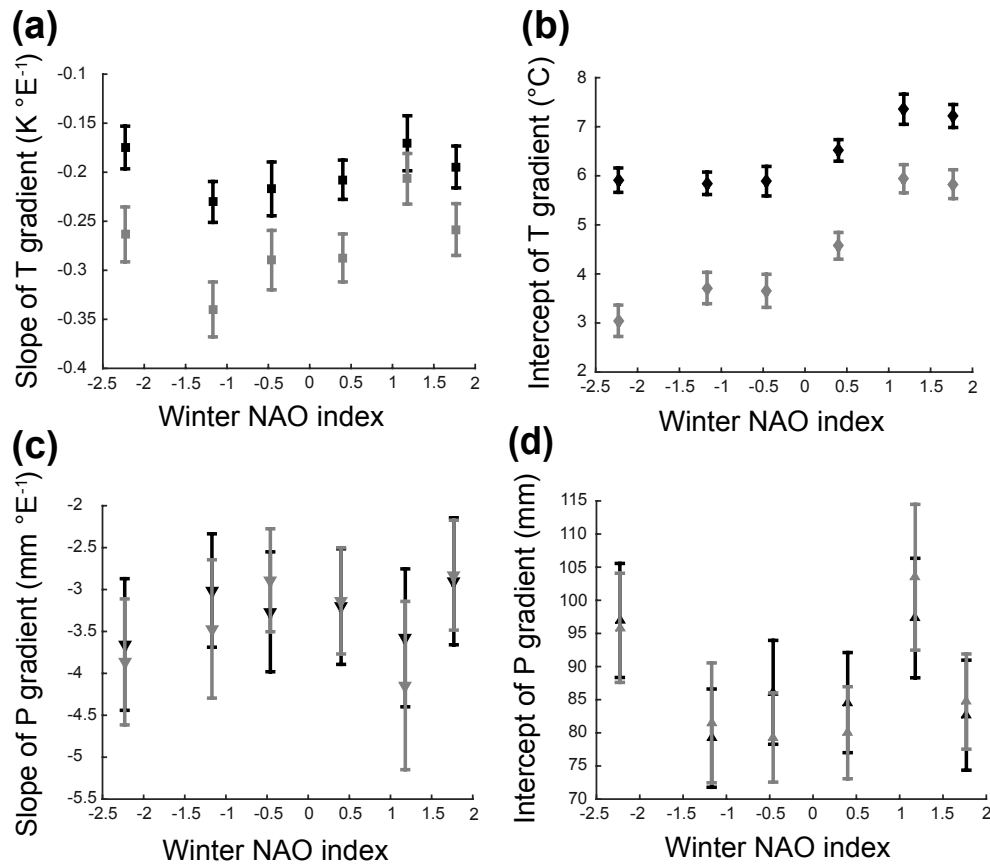


Figure 5. Based on observational data only, these four panels illustrate the slope of the continental gradient for (a) temperature and (c) precipitation as a function of the class of wNAOi that is calculated from GNIP station datasets. Panels (b) and (d) shows, respectively, the intercepts of the linear regression for the continental temperature and precipitation gradients versus the wNAOi. Black symbols indicate the results for the 6-month winter period (October–March); grey symbols denote results for the 3-month (December–February) winter period. The slopes for temperature and precipitation show no relationship with the wNAOi if all six classes are analysed ($p > 0.1$). However, omitting the most negative wNAOi class yields a significant linear correlation of 0.71 and 0.67 ($p < 0.01$) for the 6- and 3-month averages, respectively. While there is no significant relationship between the intercept of the precipitation gradients with the wNAOi ($p > 0.1$), the intercept of the air temperature gradients shows a clear trend, with lower temperatures associated with lower wNAOi values.

ference of 5.86 and 7.78 K, respectively. Hence, the average winter temperature at Valencia Observatory from October to March (December to February) is about 5.86 K (7.78 K) warmer compared to Kraków Wola Justowska for the highest wNAO class. The effect of this eastward temperature decrease can be converted into an expected $\delta^{18}\text{O}_{\text{pw}}$ and $\delta\text{D}_{\text{pw}}$ difference between the two stations. For this estimate we apply an approximate estimation of the sensitivity of $\delta^{18}\text{O}_{\text{p}}$ and $\delta\text{D}_{\text{p}}$ to temperature changes based on theoretically derived values by Dansgaard (1964), assuming a Rayleigh-type moist adiabatic condensation (vapour–liquid) process. For the sensitivity, the average value for a cooling from an initial temperature of 0 to -20°C is used, which is 0.64‰K^{-1} for $\delta^{18}\text{O}_{\text{p}}$ and 5.6‰K^{-1} for $\delta\text{D}_{\text{p}}$ (Dansgaard, 1964). Hence, for the highest wNAO class, the observed temperature difference would cause a calculated difference of 3.75 (6 months) and 4.98‰ (3 months) for $\delta^{18}\text{O}_{\text{pw}}$. $\delta^{18}\text{O}_{\text{pw}}$ values are therefore

expected to be 3.75 and 4.98‰ lighter at the easternmost station compared to the westernmost station for the 3-winter-month and 6-winter-month averages, respectively.

These theoretically calculated values are now compared with the observed differences derived from the slopes of the linear regression of the GNIP $\delta^{18}\text{O}_{\text{pw}}$ datasets (Fig. 4). For the highest wNAO class, the slope is -0.16 and $0.20\text{‰}^\circ\text{E}^{-1}$ for the 6-month and 3-month winter period. This results in an observed difference of 4.78 (6 months) and 6.02‰ (3 months). Importantly, the observed differences (longitudinal gradients) are much larger than those calculated using the air-temperature-driven Dansgaard-type model described above. The results of these calculations for $\delta^{18}\text{O}_{\text{pw}}$ and $\delta\text{D}_{\text{pw}}$, based on the observed temperature slopes and for all wNAO classes are listed in Table 1.

The most important result of this simple exercise is that the observed differences in $\delta^{18}\text{O}_{\text{pw}}$ and $\delta\text{D}_{\text{pw}}$ between the

Table 1. Differences in $\delta^{18}\text{O}_{\text{pw}}$ and $\delta\text{D}_{\text{pw}}$ (6-month (6 m) and 3-month (3 m) winter periods) between the western- (Valencia, Ireland) and easternmost station (Kraków, Poland) for all wNAOi classes based on continental GNIP station datasets. The median wNAOi for classes I to VI, respectively, are 1.77, 1.18, 0.40, -0.46 , -1.17 and -2.23 . The empirical estimates for the observed W–E difference of $\delta^{18}\text{O}_{\text{pw}}$ and $\delta\text{D}_{\text{pw}}$ presented here are based on linear regressions of the observed trends (Fig. 4). The calculated $\delta^{18}\text{O}_{\text{pw}}$ and $\delta\text{D}_{\text{pw}}$ values are based on the temperature difference between Valencia (Ireland) and Kraków (Poland) estimated from the linear regression of the continental GNIP station temperature datasets and temperature sensitivities for $\delta^{18}\text{O}_{\text{p}}$ and $\delta\text{D}_{\text{p}}$ from Dansgaard (1964). Deviation (bold numbers) means the difference between observed and calculated $\delta^{18}\text{O}_{\text{pw}}$ and $\delta\text{D}_{\text{pw}}$ values. The italic numbers state the deviation relative to the observed difference given in percentage.

wNAOi class	W–E difference for $\delta^{18}\text{O}_{\text{pw}}$								W–E difference for $\delta\text{D}_{\text{pw}}$							
	Observed		Calculated		Deviation				Observed		Calculated		Deviation			
	6 m ‰	3 m ‰	6 m ‰	3 m ‰	6 m		3 m		6 m ‰	3 m ‰	6 m ‰	3 m ‰	6 m		3 m	
				‰	%	‰	%	‰	‰	‰	‰	‰	‰	‰	%	‰
I: 1.77	4.78	6.02	3.75	4.98	1.03	22.5	1.04	17.3	42.62	52.10	32.80	43.56	9.82	23.0	8.54	16.4
II: 1.18	4.94	5.14	3.28	3.98	1.66	33.6	1.16	22.6	44.06	46.19	28.72	34.84	15.34	34.8	11.35	25.8
III: 0.40	5.73	6.32	4.00	5.54	1.73	30.2	0.79	12.5	49.37	51.68	35.01	48.44	14.36	29.1	3.24	6.3
IV: -0.46	6.66	7.89	4.18	5.58	2.48	37.2	2.31	29.3	56.93	65.10	36.58	48.81	20.35	35.7	16.29	25.0
V: -1.17	6.22	7.38	4.44	6.55	1.79	28.8	0.83	11.2	53.44	61.11	38.82	57.31	14.62	27.4	3.80	6.2
VI: -2.23	6.54	7.56	3.37	5.05	3.17	48.5	2.51	33.2	54.61	64.56	29.46	44.21	25.14	46.0	20.35	31.5

western- and easternmost GNIP stations are larger than can be accounted for by a simple air-temperature-driven Rayleigh distillation model alone (Table 1). Repeating the calculations using the sensitivity of $\delta^{18}\text{O}_{\text{pw}}$ and $\delta\text{D}_{\text{pw}}$ for the vapour–ice phase change (snow; 0.73 for $\delta^{18}\text{O}_{\text{p}}$ and 6.2 ‰ K^{-1} for $\delta\text{D}_{\text{p}}$; Dansgaard, 1964) instead results in calculated differences that are still too small to explain the observed differences in $\delta^{18}\text{O}_{\text{pw}}$ and $\delta\text{D}_{\text{pw}}$ between the western- and easternmost stations (not shown). This strongly indicates that the observed longitudinal variations in winter air temperatures alone are simply insufficient to account for the observed difference between $\delta^{18}\text{O}_{\text{pw}}$ and $\delta\text{D}_{\text{pw}}$ in western and eastern Europe and that additional processes must be considered.

Rozanski et al. (1982) pointed out that the precipitation history of air masses is an important control on observed longitudinal $\delta\text{D}_{\text{p}}$ gradients. Precipitation history can be expressed as a numerical value f (fraction of remaining moisture). Hence, f depends on the balance between the amount of precipitation (P) that has already occurred along the longitudinal gradient and the initial amount of precipitable water in the atmosphere (Q_0). However, only weak relationships are found between the precipitation gradients calculated from the GNIP station precipitation datasets and the wNAOi classes, suggesting that rainfall gradients between western and eastern Europe are fairly constant, within the range of uncertainty (Fig. 5c and d). Furthermore, the intercept of the linear regression of the precipitation data shows no dependence on the class of the wNAOi. This is consistent with the findings of Baldini et al. (2008), who showed that precipitation data from continental GNIP stations have no systematic correlation to the wNAOi (as opposed to temperature). As discussed below, this points to differences in the initial amounts of precipitable water (Q_0) as a possible

control on isotope-gradient-w–NAOi relationships (Fig. 4), over and above those attributable to air temperature gradients alone.

To better constrain the governing physical mechanisms of the precipitation history f and their first-order effects on $\delta^{18}\text{O}_{\text{pw}}$ and $\delta\text{D}_{\text{pw}}$, a simple one-box Rayleigh-type model for the atmosphere was used (Dansgaard, 1964; Eriksson, 1965):

$$\begin{aligned}
 {}^x R &= {}^x R_0 \cdot f_{\alpha-1}^x = {}^x R_0 \left(\frac{Q}{Q_0} \right)^{x\alpha-1} \\
 &= {}^x R_0 \left(1 - \frac{P}{Q_0} \right)^{x\alpha-1}.
 \end{aligned} \quad (1)$$

Equation (1) is the classic Rayleigh distillation model (Rayleigh, 1902; see also Mook, 2006 for detail) that describes the evolution of an isotope ratio R (the subscript x is a placeholder for $x=2$ (^2H) or 18 (^{18}O), i.e. for $^{18}\text{R} = ^{18}\text{O}/^{16}\text{O}$ and $^2\text{R} = ^2\text{H}/^1\text{H}$) as a function of the precipitation history f . This is a function of the amount of initial (Q_0) and remaining (Q) precipitable water in the atmosphere; Q is therefore the amount of precipitable water after a specific amount of precipitation P ($Q_0 - Q = P$) has formed. R_0 describes the initial isotope ratio. α is the equilibrium liquid–water isotope fractionation factor that depends only on temperature; the subscript x denotes, as above, the related isotope system. Because the slope of the longitudinal precipitation gradient does not change systematically with the wNAOi class, P does not change with the class of the wNAOi and has, therefore, a negligible effect on $\delta^{18}\text{O}_{\text{pw}}$ and $\delta\text{D}_{\text{pw}}$. Hence, the slope of the longitudinal gradient of $\delta^{18}\text{O}_{\text{pw}}$ and $\delta\text{D}_{\text{pw}}$ in central Europe is driven only by the temperature-dependent isotope fractionation factor α and by the initial amount of precipitable water Q_0 in the atmosphere. Although the classic Rayleigh-type model, adopted here, is

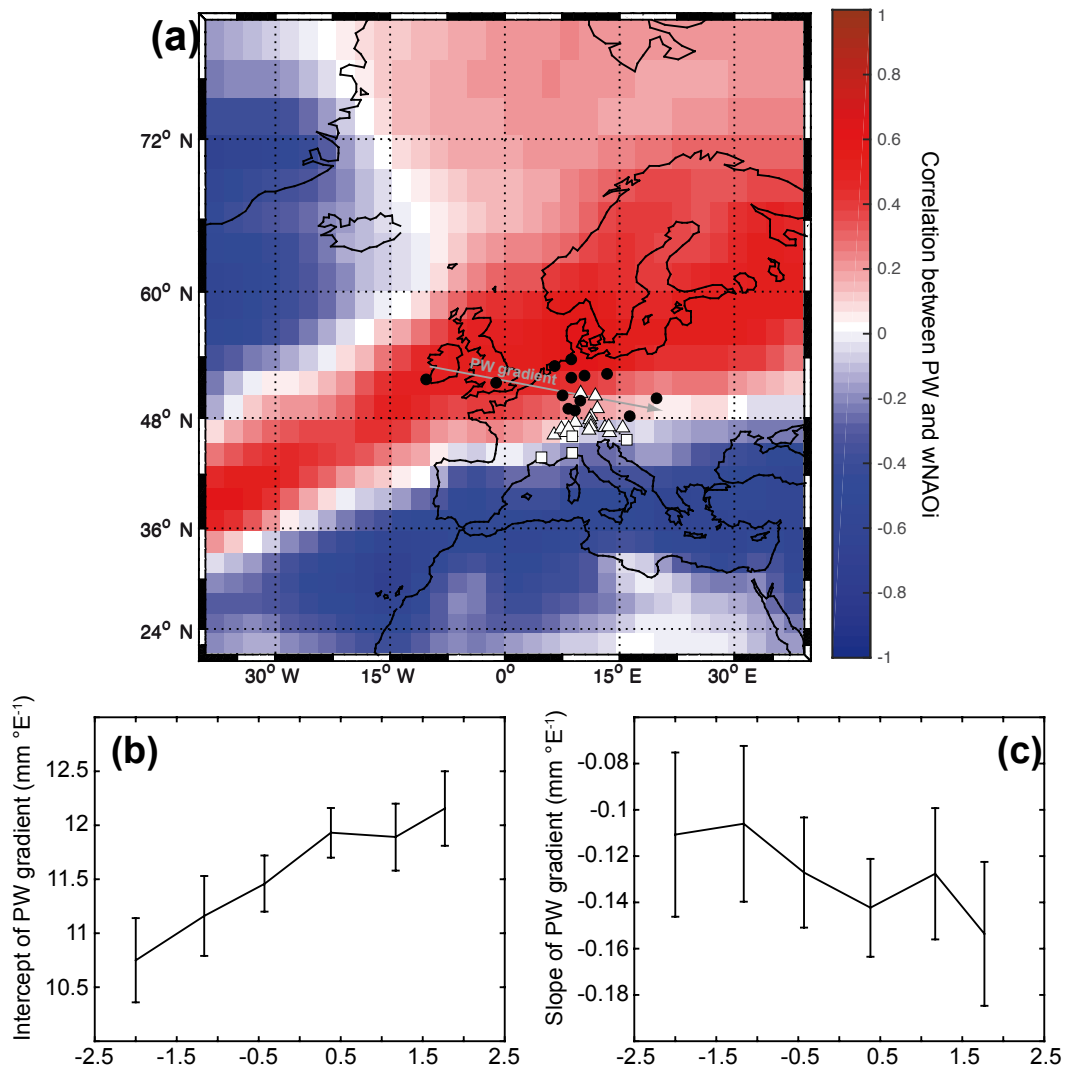


Figure 6. (a) Correlation map between the wNAOI and the amount of precipitable water (PW) for the months December to March based on NCEP/NCER reanalysis data for the period 1948–2016 and the results of the longitudinal gradient (b) intercept; (c) slope) for grid cells where continental stations are located (closed circles). Open triangles show the location of Alpine stations; open squares indicate the position of Mediterranean-influenced stations.

unable to fully capture all atmospheric processes (e.g. mixing of atmospheric moisture with different isotope signatures and/or origins), it is nonetheless a useful first approximation to explain the deviations between the calculated (temperature effect) and observed differences in $\delta^{18}\text{O}_{\text{pw}}$ and $\delta\text{D}_{\text{pw}}$ between the western- and easternmost stations. Therefore, our observations of the dependence of the longitudinal $\delta^{18}\text{O}_{\text{pw}}$ and $\delta\text{D}_{\text{pw}}$ gradient on the class of the wNAOI can be explained if, additionally, the amount of precipitable water over central Europe is lower for more negative wNAOI values. As demonstrated previously in a comparison of very positive (wNAOI > 1) and negative (wNAOI < -1) wNAOI values, the maximum amount of precipitable water in the atmosphere is shifted southward for very negative wNAOI (Trigo et al., 2002). This shift in the amount of precipitable wa-

ter is associated with changing air temperature patterns, and smaller amounts of precipitable water are associated with cooler continental air temperatures. Accordingly, our simple model shows that the atmosphere in central Europe contains less (more) atmospheric moisture during more negative (positive) wNAOI states, and this is independently supported by analysis of the amount of precipitable water in the atmosphere from an NCEP/NCER reanalysis dataset (see below). Hence, atmospheric moisture $\delta^{18}\text{O}$ and δD values are likely to be more sensitive to the rainout history during more negative wNAOI modes because f must change at a higher rate if Q_0 is smaller and P is held constant (Eq. 1). This effect is also confirmed by a multi-box exercise that assumes a Rayleigh-type condensation process, mimicking the longitudinal gradients. This multi-box exercise shows that $\delta^{18}\text{O}_{\text{p}}$ becomes

progressively depleted in dependence on Q_0 from west to east across Europe, with steeper gradients (higher slopes) for smaller Q_0 (Fig. S2).

The wNAOi–precipitable-water relationship described by Trigo et al. (2002) is also evident in the NCEP/NCER reanalysis dataset (and the ECHAM5-wiso simulations; see Supplement; Fig. 6a). The NCEP/NCER reanalysis dataset covers the period from 1948 to 2016 and is analysed for the winter months December to March; it has a spatial resolution of $2.5^\circ \times 2.5^\circ$. Precipitable water shows a positive correlation with wNAOi values in central and northern Europe (where all continental stations are located) and a negative correlation over the Mediterranean (including Iberia, the Balkans and Turkey; Fig. 6). (Interestingly, the boundary between the area of positive and negative correlation lies within the Alpine region, though the coarse resolution does not allow any detailed conclusion for individual Alpine stations.) This indicates that during positive wNAO modes, the amount of precipitable water increases over central Europe and decreases during negative wNAO modes. This finding is also confirmed by the amount of precipitable water of the analysed NCEP/NCER reanalysis grid cells (Fig. 6b and c). The results of the regression analysis of the longitudinal gradient of the precipitable water shows that the slope of the precipitable water along the longitudinal gradient is rather independent (within the range of uncertainties, although a slight trend is visible indicating a shallower slope for more negative wNAOi classes) of the wNAOi class (Fig. 6c), while the intercept clearly decreases for smaller wNAOi classes (Fig. 6b). Compared with the amount of precipitable water for the highest wNAOi class, the atmosphere contains only about 88.4 % for the lowest wNAOi class for the 6-month winter period, for example. As a result, the precipitation history f becomes more sensitive to the rainout history along the longitudinal gradient for lower wNAOi classes.

To summarize, the dependence of the observed longitudinal $\delta^{18}\text{O}_{\text{pw}}$ and $\delta\text{D}_{\text{pw}}$ gradient on the class of wNAOi in the winter season results from two processes: (i) the changing continental temperature gradients via the temperature-dependent isotope fraction during condensation, which exerts the strongest influence on the $\delta^{18}\text{O}_{\text{pw}}$ and $\delta\text{D}_{\text{pw}}$ gradient, and (ii) the dependence of the amount of precipitable water or in general of the precipitation history over central Europe on the wNAOi mode, which becomes important for more negative wNAOi classes. The latter mechanism is in agreement with recent findings of Aggarwal et al. (2012), who showed that, generally, more negative $\delta^{18}\text{O}_{\text{p}}$ values are associated with lower moisture residence times, where the moisture residence time is defined as the ratio between the amount of precipitable water and the precipitation (Aggarwal et al., 2012; Trenberth, 1998), and with conclusions of Rozanski et al. (1982), who analysed summer and winter European $\delta\text{D}_{\text{p}}$ longitudinal gradients.

4.2 Alpine stations

By comparison with the low-altitude stations, the Alpine stations reveal more complex wNAOi– $\delta^{18}\text{O}_{\text{pw}}$ and $-\delta\text{D}_{\text{pw}}$ patterns (Fig. 3). North of the Alpine divide, all stations show similar $\delta^{18}\text{O}_{\text{pw}}$ – and $\delta\text{D}_{\text{pw}}$ –wNAOi class relationships as at the Garmisch-Partenkirchen GNIP station (Fig. 2). The only exception to this relationship is the $\delta^{18}\text{O}_{\text{pw}}$ datasets for Thonon-les-Bains, whose $\delta^{18}\text{O}_{\text{pw}}$ datasets have only a weak relationship with the wNAOi. The relationship between the $\delta^{18}\text{O}_{\text{pw}}$ – $\delta\text{D}_{\text{pw}}$ values and wNAOi from stations at and south of the Alpine divide, including Grimsel (no. 18; western Alps); Längenfeld (no. 21), Obergurgl (no. 23), Patscherkofel (no. 27; all central Alps); Böckstein (no. 30), St. Peter (no. 31), Villacher Alpe (no. 32) and Graz (no. 33; eastern Alps) is more complex compared to the stations north of the Alpine divide (see Sect. 3.2 for details).

The $\delta^{18}\text{O}_{\text{pw}}$, $\delta\text{D}_{\text{pw}}$, temperature and precipitation datasets were also grouped into six wNAOi classes according to wNAOi as previously for the non-Alpine stations (Sect. 4.1). A detailed analysis of the $\delta^{18}\text{O}_{\text{pw}}$ and $\delta\text{D}_{\text{pw}}$ values of all Alpine stations shows that the median $\delta^{18}\text{O}_{\text{pw}}$ values become more negative for higher altitudes, irrespective of the wNAOi class. This observation is well known as the “altitude effect” (Dansgaard, 1954; Schürch et al., 2003). However, there is no obvious relationship ($p > 0.1$ for all datasets) between the class of the wNAOi and the altitude effect for the Alpine stations (Fig. 7a and b). On average, the altitude effect is $-0.32\text{‰ } 100\text{ m}^{-1}$ (6-month average) and $-0.30\text{‰ } 100\text{ m}^{-1}$ (3-month average) for $\delta^{18}\text{O}_{\text{pw}}$ and $-2.55\text{‰ } 100\text{ m}^{-1}$ (6-month average) and $-2.28\text{‰ } 100\text{ m}^{-1}$ (3-month average) for $\delta\text{D}_{\text{pw}}$ (Fig. 7a and b). Furthermore, the recorded air temperature at the Alpine stations changes on average by about -0.58 and $-0.56\text{ K } 100\text{ m}^{-1}$ for the 6-month and 3-month average, respectively, independent of the wNAOi class ($p > 0.1$ for all datasets; Fig. 7c). The mean values of the temperature–altitude relationship correspond approximately to the moist adiabatic lapse rate. Hence, a strong relationship between $\delta^{18}\text{O}_{\text{pw}}$ and $\delta\text{D}_{\text{pw}}$ values and air temperature is observed in the Alpine stations (e.g. Schürch et al., 2003). No relationship between rainfall amount and $\delta^{18}\text{O}_{\text{pw}}$ was observed (Fig. 7d).

Because there is no relationship between the lapse rate and/or precipitation amount with the wNAOi class, we conclude that the observed relationships between $\delta^{18}\text{O}_{\text{pw}}$ and $\delta\text{D}_{\text{pw}}$ and the class of the wNAOi for our selection of Alpine stations are (i) caused by different air mass origins linked to wNAOi states and (ii) downstream effects of the varying central European continental effect that causes more negative $\delta^{18}\text{O}_{\text{pw}}$ and $\delta\text{D}_{\text{pw}}$ values for more negative wNAOi classes. The weak or absent relationships for stations at the Alpine divide can be caused by air masses of different origins (e.g. variable influences of the Mediterranean-sourced moisture; Kaiser et al., 2001). However, detailed back trajectories of rainfall events for the entire Alpine region would be required

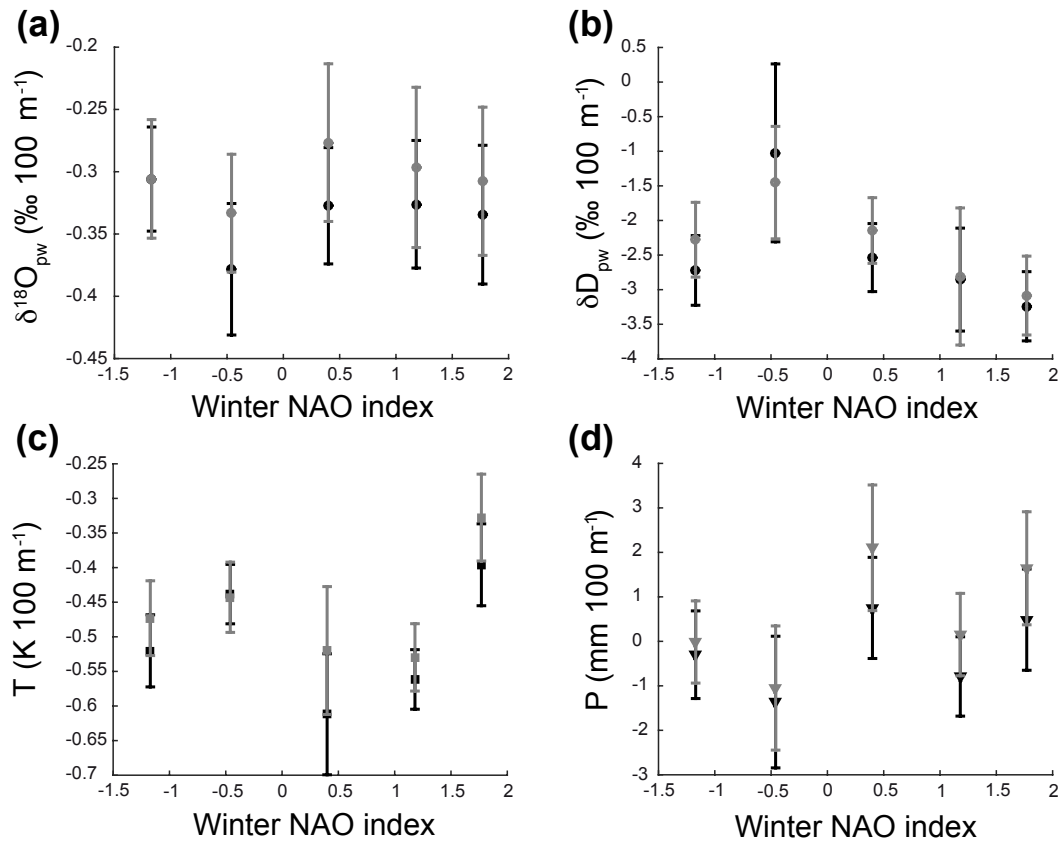


Figure 7. The four panels show the rate of change of (a) $\delta^{18}\text{O}_{\text{pw}}$, (b) $\delta\text{D}_{\text{pw}}$, (c) temperature (T) and (d) precipitation (P) as a function of altitude for different wNAOi classes. (The lowest wNAOi class was not analysed because data of only four stations (out of 17) are available.) All Alpine stations are included. None of the correlations are statistically significant ($p > 0.1$). Black symbols indicate the results of the 6-month winter period; grey symbols denote the 3-month winter period.

to further evaluate this explanation. Our analysis indicates that the Alpine divide exerts an important influence on the winter hydrological cycle in the region, with precipitation north of the Alps sourced by atmospheric moisture originating from central Europe. In winter, this residual atmospheric moisture is already depleted in ^{18}O and ^2H when it reaches the northern part of the Alps, reflecting the ambient winter mode of the wNAOi and thereby determining the degree of the depletion in ^{18}O and ^2H in north Alpine winter precipitation.

To complete the above conclusion on the mixing of atmospheric moisture for stations at the Alpine divide, the $\delta^{18}\text{O}_{\text{pw}}$ and $\delta\text{D}_{\text{pw}}$ of circum-Mediterranean stations were also analysed for their dependence on the wNAOi (a discussion of the NAO relationships between $\delta^{18}\text{O}_{\text{pw}}$ and $\delta\text{D}_{\text{pw}}$ and temperature and precipitation can be found in the Supplement). These stations are Avignon (34; southwest of the Alps), Locarno (35; south of Grimsel), Genoa (Setri; south of the Alps; 36) and Zagreb (37; southeast of the Alps; Fig. 1). For the 3-month $\delta^{18}\text{O}_{\text{pw}}$ and $\delta\text{D}_{\text{pw}}$, only data from Avignon and Zagreb show a strong relationship with the wNAOi (about 1 ‰/wNAOi unit for $\delta^{18}\text{O}_{\text{pw}}$; Fig. 3a and c). For the 6-month

$\delta^{18}\text{O}_{\text{pw}}$ and $\delta\text{D}_{\text{pw}}$ data, only the $\delta^{18}\text{O}_{\text{pw}}$ dataset from Locarno and the $\delta^{18}\text{O}_{\text{pw}}$ and $\delta\text{D}_{\text{pw}}$ datasets from Zagreb show a relationship with wNAOi. The NAO relationships of $\delta^{18}\text{O}_{\text{pw}}$ and $\delta\text{D}_{\text{pw}}$ for the 3-month winter period from the Mediterranean stations Locarno and Genoa (Setri) show that the NAO fingerprint, which is observed for Alpine stations north of the Alpine divide, is not transferred to these two stations. The situation might change for $\delta^{18}\text{O}_{\text{pw}}$ from Locarno for the 6-month winter period where a relationship with the wNAOi is observed. The stronger relationship for this winter period could be caused by an increase in precipitation that results from air masses from central Europe. For Zagreb, it is difficult to explain the observed relationships between $\delta^{18}\text{O}_{\text{pw}}$ and $\delta\text{D}_{\text{pw}}$ because the closest Alpine stations show no relationship with the wNAOi. To further investigate the mechanisms that control the $\delta^{18}\text{O}_{\text{pw}}$ and $\delta\text{D}_{\text{pw}}$ datasets in Avignon and Zagreb, the origin of the air masses in dependence on the wNAOi needs to be investigated further using isotope-enabled regional climate models to better constrain the effect of local temperature and precipitation on $\delta^{18}\text{O}_{\text{pw}}$ and $\delta\text{D}_{\text{pw}}$. In summary, the variable wNAO relationship of $\delta^{18}\text{O}_{\text{pw}}$ and $\delta\text{D}_{\text{pw}}$ datasets from the investigated Mediterranean stations

support the observation that the Alpine divide represents an important boundary region for the oxygen and hydrogen isotope system of Alpine precipitation.

5 Implications for palaeoclimate reconstructions from speleothems

5.1 Reconstructions from single speleothem-based carbonate $\delta^{18}\text{O}$

The results have important implications for palaeoclimate archives that record the $\delta^{18}\text{O}_{\text{pw}}$ and $\delta\text{D}_{\text{pw}}$ values of winter precipitation (October to March, the main period of infiltration in central Europe due to low evapotranspiration rates). Potentially, such archives include speleothems and groundwater. The following discussion focuses on speleothem carbonate $\delta^{18}\text{O}$ records but is also applicable to speleothem fluid inclusion $\delta^{18}\text{O}$ and δD records and is relevant for other palaeoclimate archives.

For a paleoclimate reconstruction that is based on a single speleothem from a cave site from central Europe or north of the Alpine divide, $\delta^{18}\text{O}_{\text{pw}}$ and $\delta\text{D}_{\text{pw}}$ values are typically lower for more negative wNAOi values (Fig. 3). The median sensitivity of $\delta^{18}\text{O}_{\text{pw}}$ from all continental stations is 0.57‰ per wNAOi unit. Hence, a persistent change in the average wNAOi from, e.g., +1 to −1 (i.e. −2 wNAOi units) would result in a reduction in the average $\delta^{18}\text{O}_{\text{pw}}$ by 1.14‰. Furthermore, monthly average air temperatures are generally in phase with the wNAOi changes, resulting in a positive linear relationship between $\delta^{18}\text{O}_{\text{pw}}$ and $\delta\text{D}_{\text{pw}}$ and air temperatures. Hence, air temperatures tend to be lower depending on the cave location if the average wNAOi is smaller. This temperature relationship was used recently to reconstruct historic $\delta^{18}\text{O}_{\text{pw}}$ values (Mischel et al., 2015), and its use has been suggested for wNAOi reconstructions (Casado et al., 2013). Crucially, however, the $\delta^{18}\text{O}_{\text{pw}}$ and $\delta\text{D}_{\text{pw}}$ variability is controlled not only by changes in air temperature but also by changes in the air mass precipitation history (Sect. 4). Hence, the use of speleothem $\delta^{18}\text{O}$ values (or $\delta^{18}\text{O}$ and δD values from fluid inclusions or groundwater) to directly reconstruct the past variability of the wNAOi or winter temperatures should be undertaken cautiously because past changes in the hydrological cycle could result in a relationship between $\delta^{18}\text{O}_{\text{pw}}$ and temperature that differs from the present day. This is particularly important for long-term reconstructions of atmospheric circulation. As for the case of individual speleothem $\delta^{18}\text{O}$ records, caution should be exercised when interpreting changes in $\delta^{18}\text{O}$ gradients inferred from multi-speleothem regression analysis because the continental precipitation $\delta^{18}\text{O}_{\text{pw}}$ and $\delta\text{D}_{\text{pw}}$ gradients are controlled by both the air temperature gradient and the air mass precipitation history (Sect. 4).

Notwithstanding these caveats, the results from the sensitivity analysis of $\delta^{18}\text{O}_{\text{pw}}$ and air temperature theoretically allow estimates of the possible influences of changes in

$\delta^{18}\text{O}_{\text{pw}}$ and temperature for wNAOi changes on speleothem $\delta^{18}\text{O}$ records. For this exercise we use the station data of Stuttgart (Canstatt; no. 8), located in southern Germany with a $\delta^{18}\text{O}_{\text{pw}}$ -wNAOi sensitivity similar to the median of all continental stations. For the period from October to March, the NAO–temperature relationship for this station suggests a sensitivity of 0.63 K/wNAOi unit and an intercept of 4.38 °C ($r = 0.57$); no NAO relationship is observed for precipitation amount. In the example above, a decrease in the NAO index from +1 to −1 would cause a change of −1.20‰ in $\delta^{18}\text{O}_{\text{pw}}$ in Stuttgart precipitation, with a concomitant decrease in air temperature of approximately 1.26 K. Assuming that these changes in $\delta^{18}\text{O}_{\text{pw}}$ and air temperature on the surface are transmitted into a cave, we can estimate both effects on speleothem $\delta^{18}\text{O}$ values. However, this is only reasonable for persistent changes in the NAO on decadal to millennial timescales when there is sufficient time for thermal equilibration of the cave air temperature to changes in the surface air temperature and where any annual variability of the wNAO (i.e. “noise”) is overwhelmed by the persistent change in the wNAO (“signal”).

Applying the temperature sensitivity of the equilibrium oxygen-isotope fractionation factor of Kim and O’Neil (1997) of about -0.22‰ K^{-1} , the temperature change of −1.26 K would result in an increase in speleothem $\delta^{18}\text{O}$ by about +0.28‰, but the simultaneous decrease by 1.20‰ in drip water $\delta^{18}\text{O}$ would dominate, resulting in an overall decrease in the speleothem $\delta^{18}\text{O}$ by about 0.92‰. Therefore, the changes in precipitation $\delta^{18}\text{O}_{\text{pw}}$ would dominate the speleothem $\delta^{18}\text{O}$ record. We stress that these idealized conditions are rarely met in natural cave systems where other processes typically influence the speleothem proxy values (e.g. isotope disequilibrium effects; Deininger et al., 2012). Nonetheless, this exercise emphasizes that the sensitivity of $\delta^{18}\text{O}_{\text{pw}}$ to wNAOi is great and that persistent changes (i.e. centennial and millennial changes) in the mean state of the wNAO are likely to produce detectable and coherent changes in speleothem $\delta^{18}\text{O}$ time series in central Europe.

It is notable that for speleothems deposited in caves close to the Alpine divide where there is little or no relationship between $\delta^{18}\text{O}_{\text{pw}}$ and the wNAOi, speleothem $\delta^{18}\text{O}$ values are likely to be dominated by the temperature-dependent isotope fractionation factor during speleothem growth rather than by changes in $\delta^{18}\text{O}_{\text{pw}}$. Hence, if modern/historic temperature calibrations of speleothem $\delta^{18}\text{O}$ values are conducted, a relatively straightforward, but site-specific negative correlation between speleothem $\delta^{18}\text{O}$ and temperature is to be expected for sites close to the Alpine divide. This inference is supported by the two currently available studies: one at Spannagel Cave, Austria, which is located close to the Alpine divide in the central Alps where the temperature calibration is -0.44‰ K^{-1} (Mangini et al., 2005), and one from Milandre Cave situated in the Swiss Jura Mountains (western Alps) approximately 150 km north of the Alpine divide, where the temperature calibration is 0.70‰ K^{-1} (D. Fleitmann, 2016,

personal communication). Taking the temperature sensitivity of $\delta^{18}\text{O}_{\text{pw}}$ of about 0.95‰ K^{-1} for the GNIP station Konstanz, located at a similar latitude as Milandre Cave, and the temperature sensitivity of the equilibrium isotope fractionation between water and calcite of about -0.22‰ K^{-1} , yields a net value of 0.73‰ K^{-1} . This value is broadly consistent with the temperature calibration (0.70‰ K^{-1}) found for Milandre Cave by Fleitmann.

The above discussion focused only on changes in $\delta^{18}\text{O}_{\text{pw}}$ and temperature that are transmitted into the cave. However, in natural cave systems, other environmental parameters linked to persistent changes in the wNAO could also influence speleothem $\delta^{18}\text{O}$. These include parameters such as cave air CO_2 concentrations ($p\text{CO}_2$), the Ca^{2+} concentration of drip waters or drip intervals. Modelling (e.g. Deininger et al., 2012; Mühlinghaus et al., 2009) and experimental work (e.g. Polag et al., 2010; Wiedner et al., 2008; Day and Henderson, 2011) reveal that these parameters can influence speleothem (calcite) $\delta^{18}\text{O}$ via isotope disequilibrium effects. These latter effects can in principle be as large as the NAO-related changes calculated above (see Deininger et al., 2012, for a thorough discussion on the sensitivity of all these parameters). Therefore, such reconstructions should be always undertaken cautiously because they can include large uncertainties. Furthermore, $\delta^{18}\text{O}_{\text{pw}}$ variability can be smoothed during water percolation through the karst system, resulting in fairly constant drip water $\delta^{18}\text{O}$ values, which may further influence speleothem $\delta^{18}\text{O}$ (Mischel et al., 2015). The effects of these complications can be minimized through the use of well-monitored cave systems where the “modern” (meaning over the duration of the monitoring period) cave system and the response of the diverse parameters monitored to natural changes in the surface conditions are well constrained, combined with appropriate forward models (e.g. ISOLUTION, Deininger et al., 2012) that allow estimates of the magnitude of these effects on speleothem $\delta^{18}\text{O}$. Furthermore, the use of multiple coeval speleothem records from different cave systems can be regarded as a potential (new) approach to synthesize the common signal of all of these records (e.g. $\delta^{18}\text{O}$) using for example principal component analysis (Deininger et al., 2016) or other statistical techniques (Rehfeld et al., 2013; Fischer, 2016).

5.2 Multiple speleothem-based reconstructions of Holocene longitudinal speleothem $\delta^{18}\text{O}$ gradients and implication of the evolution of the North Atlantic Oscillation

Although the aforementioned processes can modify speleothem $\delta^{18}\text{O}$ values, their effects might be negligible or at least less important when the palaeoclimate signals of multiple coeval speleothem $\delta^{18}\text{O}$ records are used to reconstruct past climate dynamics. As an example, McDermott et al. (2011) used $\delta^{18}\text{O}$ data for several coeval speleothems to show that longitudinal speleothem $\delta^{18}\text{O}$ gradients across

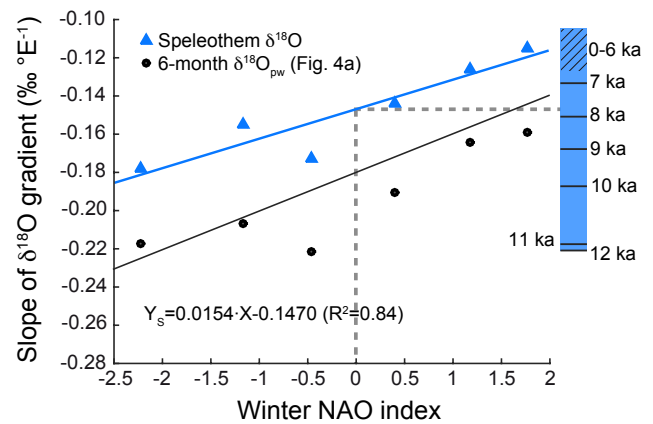


Figure 8. The blue triangles illustrate the forward-modelled longitudinal slopes for speleothem records calculated for each wNAOI class from their respective 6-month (October–March) longitudinal $\delta^{18}\text{O}_{\text{pw}}$ gradients (closed circles) and the observed temperature gradient converted into a speleothem $\delta^{18}\text{O}$ gradient using a sensitivity of 0.225‰ K^{-1} (Kim and O’Neil, 1997). The blue and black line indicates the regression line from the longitudinal speleothem $\delta^{18}\text{O}$ and $\delta^{18}\text{O}_{\text{pw}}$ gradient, respectively. The blue bar highlights the range of reconstructed longitudinal speleothem $\delta^{18}\text{O}$ slopes during the Holocene (McDermott et al., 2011). The temporal evolution of the speleothem $\delta^{18}\text{O}$ slopes (McDermott et al. (2011) varies between -0.2208 and -0.1336‰ ° E^{-1} from 12 ka to 7 ka and varies between -0.1266 and -0.1046‰ ° E^{-1} from 6 ka to the present (shaded area). Comparison of the speleothem slopes with those calculated in this study suggests predominantly wNAO– like modes in the early Holocene until about ca. 8 ka and wNAO+ like modes in the mid and late Holocene.

Europe changed systematically during the Holocene. To compare the observed slopes and their temporal evolution during the Holocene and to evaluate a possible NAO-like mechanism, the 6-month (October–March) longitudinal $\delta^{18}\text{O}_{\text{pw}}$ gradients need to be converted into expected speleothem (calcite) $\delta^{18}\text{O}$ gradients. Such estimates require that both the longitudinally variable winter temperature gradients (Fig. 5a) as well as the $\delta^{18}\text{O}_{\text{pw}}$ slopes (Fig. 4a) are taken into account. The effects of varying temperature gradients are considered via the temperature-dependent oxygen isotope fractionation between water and calcite. These estimates show that the slope of the longitudinal speleothem $\delta^{18}\text{O}$ gradient is expected to be greatest for the highest wNAOI class, decreasing for lower wNAOI classes. The calculated slopes for speleothem calcite based on the longitudinal $\delta^{18}\text{O}_{\text{pw}}$ slopes and air temperature gradients of this study show remarkable agreement with a recent reconstruction of speleothem-based $\delta^{18}\text{O}$ gradients throughout the Holocene (McDermott et al., 2011), (Fig. 8).

Assuming that the present-day mechanisms that determine the observed relationships between the wNAOI and temperature, precipitation and $\delta^{18}\text{O}_{\text{pw}}$ are relevant for the boreal winter of the entire Holocene, the evolution of the recon-

structured Holocene speleothem $\delta^{18}\text{O}$ gradients can be interpreted as reflecting changes in atmospheric pressure patterns akin to predominantly negative wNAOi-like modes in the early Holocene until about ca. 8 ka and mainly positive wNAOi-like modes during mid and late Holocene winters (this assumption includes caveats that are discussed further below). For this assumption (NAO type forcing), the changes in the speleothem $\delta^{18}\text{O}$ gradients are caused by changing temperature gradients (steeper west-to-east European temperature gradients in the early Holocene) and a changing precipitation history (increased precipitation and/or reduced amount of moisture in the atmosphere) linked to an NAO-like forcing. However, this interpretation requires that the NAO was operating akin to modern observations. In other words: it hypothesizes that the Azores High and the Icelandic Low were broadly stationary in space and time. A recent study has demonstrated recent (1871–2008 AD) non-stationarity of the Azores High (AH) and the Icelandic Low (IL), (expressed as the NAO angle index, which is positive when the IL is east of the AH and vice versa), but the latter is correlated with the wNAOi: a positive angle index tends to coincide with a positive wNAOi (Wang et al., 2012). For the Holocene, stationarity is hypothesized for the last 8 kyr by Wassenburg et al. (2016), who proposed that the NAO reorganized between 9 and 8 kyr ago in response to the melting Laurentide Ice Sheet and meltwater fluxes into the North Atlantic (Wassenburg et al., 2016). This study further suggests that the Icelandic Low was shifted southwest of its modern position during the early Holocene. The timing of this NAO reorganization would be consistent with the finding of this study that the NAO switched from predominantly negative to positive wNAOi at about 8 ka. However, in contrast to the findings of Wassenburg et al. (2016), our study based on the results of McDermott et al. (2011) would suggest a gradual shift in the IL and/or AH towards the northeast or southwest, respectively, during the course of the Holocene until stable boundary conditions are reached 5 to 4 kyr ago.

The different inferences in this study (and that of McDermott et al., 2011) and Wassenburg et al. (2016) may be that the observations of Wassenburg et al. (2016) are based on two stalagmite proxy records only, located in northern Germany and northern Morocco, which are sensitive to the local amount of precipitation. The modern precipitation amount of the two regions is driven mainly by the NAO but with opposite correlations: positive in northern Germany and negative in northern Morocco (cf. Fig. 1b in Wassenburg et al., 2016). Hence, if these two speleothem precipitation-proxy records were compared from these two regions, we would expect that, if the modern precipitation regimes had not changed, these two proxy records would be anti-correlated. If, however, the modern precipitation regimes changed (e.g. they shifted in response to changes in the atmospheric circulation) and if the local precipitation amount at the two locations changed in the same direction, the two proxy records should be correlated. This scenario is exactly observed by

Wassenburg et al. (2016), who show that the correlation between these two speleothem proxy records from northern Germany and northern Morocco changed from positive to negative between 9 ka and 8 ka (see Wassenburg et al., 2016, for details). However, the correlation of these two records is only a local perspective on the history of the amount of precipitation at these two individual locations and cannot resolve gradual changes in the precipitation pattern; it can only indicate whether the locations lie within the same hydrological regime or not. By contrast, the results of McDermott et al. (2011) that are further evaluated by this study are based on multiple speleothem $\delta^{18}\text{O}$ records that are distributed throughout Europe and are potentially more reliable for detecting gradual changes. However, we emphasize that the results of our study and those of Wassenburg et al. (2016) do not contradict, but rather complement each others and give two different views on the same phenomenon, a gradual change in the NAO during the Holocene that is likely caused by a relative shift in the IL and AH, mimicking NAO-like conditions in the speleothem $\delta^{18}\text{O}$ gradients. The conclusion of the aforementioned studies and the results presented here is that the relative location of the IL and AH changed gradually during the Holocene: in the early Holocene the IL and/or the AH were located southwest and northeast, respectively, of their modern positions, eventually mimicking negative NAO-like conditions; subsequently, the location shifted northeastwards and southwestwards, respectively, during the Holocene, mimicking positive and modern NAO-like conditions, consistent with an independent study from the Iberian Peninsula (Walczak et al., 2015). This gradual change was potentially forced by the retreat of the Laurentide Ice Sheet during the early Holocene (Wassenburg et al., 2016) and possibly also by the changing Holocene wintertime insolation (McDermott et al., 2011; Walczak et al., 2015).

The approach applied by this study uses modern relationships between longitudinal precipitation $\delta^{18}\text{O}_{\text{pw}}$ gradients and the wNAOi and argues that the observed changes are caused (i) by changing temperature gradients between west and east Europe and (ii) a modified precipitation history f that accounts for changes in the amount of precipitable water in the atmosphere and in principle changing precipitation amounts. Though the latter (changes in the precipitation amount) was not evident in the analysed station datasets, there is no reason to exclude it for the Holocene interpretation of changing longitudinal speleothem $\delta^{18}\text{O}$ gradients. This approach includes several caveats that need to be discussed in more detail. First, modern relationships are derived for yearly winter values (6-month and 3-month average values) that are derived mainly post AD 1961 (when the GNIP network began). (The ECHAM5-wiso simulations used here also cover only the post AD 1960 period.) However, in this period, the NAO angle index was fairly stable and the relative location of the AH and IL did not vary much compared to the period before (Wang et al., 2012). Hence, we cannot rule out any effect of the relative location of the AH and IL on

the modern relationships between longitudinal $\delta^{18}\text{O}_{\text{pw}}$ gradients and the NAO, and the conversion of the speleothem $\delta^{18}\text{O}$ gradients into wNAOi should be interpreted cautiously. Furthermore, recent studies have also highlighted that other atmospheric pressure systems (like the east Atlantic pattern) also exert an influence on European $\delta^{18}\text{O}_{\text{p}}\text{--NAO}$ relationships (Comas-Bru et al., 2016) but did not study its relationship with the angle index of the NAO. This would, however, be interesting because there might be relationships between the strength and location of the east Atlantic pattern and the angle index of the NAO (i.e. with the relative location between the AH and the IL). Second, a requirement for the interpretation of the changing longitudinal speleothem $\delta^{18}\text{O}$ gradients as variations of the NAO is a time-stationary NAO depiction back to the early Holocene. However, this requirement can be questioned based on the recent findings of Walczak et al. (2015) and Wassenburg et al. (2016), who demonstrated Holocene shifts in the AH and IL. Their conclusion is further supported by this study. Hence, the gradual shift in the speleothem $\delta^{18}\text{O}$ gradients during the Holocene should be interpreted as relative shifts in the AH and IL that are akin to the modes of the modern NAO (i.e. NAO-like) but likely have very different (ice sheets, insolation) forcing mechanisms on these longer timescales. Further research is necessary to illuminate these caveats, extending, on the one hand, palaeoclimate investigations to generate new palaeoclimate proxy records and, on the other hand, conducting climate model simulations to study in detail the relationships between the dominating pressure systems and palaeoclimate proxy records as well as their underlying mechanism.

6 Conclusions and summary

This study investigated the relationships between central European and Alpine $\delta^{18}\text{O}_{\text{pw}}$ and $\delta\text{D}_{\text{pw}}$ values and the North Atlantic Oscillation index for the boreal winter (wNAOi). $\delta^{18}\text{O}_{\text{pw}}$ and $\delta\text{D}_{\text{pw}}$ data for 37 meteorological stations distributed over central Europe and the Alps were analysed. This study demonstrates that the European continental isotope effect depends on the wNAOi, with steeper $\delta^{18}\text{O}_{\text{pw}}$ gradients associated with more negative wNAOi values. Hence, precipitation $\delta^{18}\text{O}_{\text{pw}}$ and $\delta\text{D}_{\text{pw}}$ values across central Europe are more negative for lower wNAOi winters. We argue that the strength of this change is caused by (i) a steeper west-to-east continental air temperature gradient and (ii) a decrease in the precipitable water content of the atmosphere during more negative wNAOi conditions. (An evaluation of the longitudinal $\delta^{18}\text{O}_{\text{pw}}$ and $\delta\text{D}_{\text{pw}}$ gradients from an isotope-enabled general circulation model, ECHAM5-wiso, shows that the simulated slopes are well reproduced compared with those reconstructed from observational data).

The emerging picture for Alpine stations is that for stations north of the alpine divide, $\delta^{18}\text{O}_{\text{pw}}$ and $\delta\text{D}_{\text{pw}}$ values show a similar relationship with the wNAOi as continental stations

north of the Alps. However, in contrast with the processes that determine $\delta^{18}\text{O}_{\text{pw}}$ and $\delta\text{D}_{\text{pw}}$ values at continental stations, $\delta^{18}\text{O}_{\text{pw}}$ and $\delta\text{D}_{\text{pw}}$ characteristics at Alpine stations are mainly a downstream residual effect of the changing continental effect. Furthermore, $\delta^{18}\text{O}_{\text{pw}}$ and $\delta\text{D}_{\text{pw}}$ values of stations close to the Alpine divide in the central and eastern Alps exhibit a weak or absent relationship with the wNAOi. The results of this study have important implications for palaeoclimate reconstructions that are based on winter $\delta^{18}\text{O}_{\text{pw}}$ and $\delta\text{D}_{\text{pw}}$ values, such as speleothem $\delta^{18}\text{O}$ records.

A simplistic interpretation of recent findings on the temporal evolution of longitudinal speleothem $\delta^{18}\text{O}$ gradients, assuming that modern NAO-related mechanisms are relevant for the Holocene, would be that the early Holocene was characterized by more negative NAO-like modes, while the mid and late Holocene would be characterized by more positive NAO-like modes. However, consistent with other independent studies (Wassenburg et al., 2016; Walczak et al., 2015) and an augmented NAO index that accounts for the relative position of the Azores High (AH) and Icelandic Low (IL; Wang et al., 2012), we interpret the observed gradual Holocene change in longitudinal speleothem $\delta^{18}\text{O}$ gradients as a relative shift in the angular position of the AH and IL. These positions eventually evolve to situations akin to modern positive and negative NAO modes, but the millennial forcing mechanisms during the course of the Holocene are likely to be different from the present-day inter-annual to decadal variability. Further observational and modelling studies are necessary to better constrain the complex relationships between the atmospheric circulation and palaeoclimate proxy records.

7 Data availability

The processed data are available through the Supplement. Unprocessed data can be accessed at http://www.naweb.iaea.org/naweb/ih/IHS_resources_gnip.html and <https://wasser.umweltbundesamt.at/h2odb/>.

The Supplement related to this article is available online at doi:10.5194/cp-12-2127-2016-supplement.

Acknowledgements. We thank all operating organizations of the Global Network of Isotopes in Precipitation (GNIP) and the Austrian Network of Isotopes in Precipitation (ANIP) and all contributing researchers for their efforts to run and maintain the stations, which made this study possible. We are grateful to three anonymous reviewers for their constructive comments that helped to improve the paper and to the associated editor Dominik Fleitmann for handling our paper. Michael Deininger is funded by the Irish Research Council (IRC) by a Government of Ireland Postdoctoral Fellowship (GOIPD/2015/789). Frank McDermott

acknowledges support from Science Foundation Ireland through its Research Frontiers Program (RFP) Grants 07/RFP/GEOF265 and 08/FRP/GEO1184.

Edited by: D. Fleitmann

Reviewed by: three anonymous referees

References

- Aggarwal, P. K., Alduchov, O. A., Froehlich, K. O., Araguas-Araguas, L. J., Sturchio, N. C., and Kurita, N.: Stable isotopes in global precipitation: A unified interpretation based on atmospheric moisture residence time, *Geophys. Res. Lett.*, **39**, L11705 doi:10.1029/2012GL051937, 2012.
- Baldini, L. M., McDermott, F., Foley, A. M., and Baldini, J. U. L.: Spatial variability in the European winter precipitation $\delta^{18}\text{O}$ -NAO relationship: Implications for reconstructing NAO-mode climate variability in the Holocene, *Geophys. Res. Lett.*, **35**, L04709, doi:10.1029/2007GL032027, 2008.
- Barnston, A. G. and Livezey, R. E.: Classification, seasonality and persistence of low-frequency atmospheric circulation patterns, *Mon. Weather Rev.*, **115**, 1083–1126, 1987.
- Casado, M., Ortega, P., Masson-Delmotte, V., Risi, C., Swingedouw, D., Daux, V., Genty, D., Maignan, F., Solomina, O., Vinther, B., Viovy, N., and Yiou, P.: Impact of precipitation intermittency on NAO-temperature signals in proxy records, *Clim. Past*, **9**, 871–886, doi:10.5194/cp-9-871-2013, 2013.
- Comas-Bru, L. and McDermott, F.: Impacts of the EA and SCA patterns on the European twentieth century NAO-winter climate relationship, *Q. J. Roy. Meteorol. Soc.*, **140**, 354–363, doi:10.1002/qj.2158, 2013.
- Comas-Bru, L., McDermott, F., and Werner, M.: The effect of the East Atlantic pattern on the precipitation $\delta^{18}\text{O}$ -NAO relationship in Europe, *Clim. Dynam.*, **47**, 2059–2069, 2016.
- Craig, H.: Isotopic variations in meteoric waters, *Science*, **133**, 1702–1703, 1961.
- Craig, H. and Gordon, L. I.: Deuterium and oxygen 18 variations in the ocean and the marine atmosphere, Consiglio nazionale delle ricerche, Laboratorio de geologia nucleare, 1965.
- Dansgaard, W.: The O 18-abundance in fresh water, *Geochim. Cosmochim. Ac.*, **6**, 241–260, 1954.
- Dansgaard, W.: Stable isotopes in precipitation, *Tellus*, **16**, 436–468, 1964.
- Day, C. C. and Henderson, G. M.: Oxygen isotopes in calcite grown under cave-analogue conditions, *Geochim. Cosmochim. Ac.*, **75**, 3956–3972, 2011.
- Deininger, M., Fohlmeister, J., Scholz, D., and Mangini, A.: Isotope disequilibrium effects: The influence of evaporation and ventilation effects on the carbon and oxygen isotope composition of speleothems-A model approach, *Geochim. Cosmochim. Ac.*, **96**, 57–79, doi:10.1016/j.gca.2012.08.013, 2012.
- Deininger, M., McDermott, F., Mudelsee, M., Werner, M., Frank, N., and Mangini, A.: Coherency of late Holocene European speleothem $\delta^{18}\text{O}$ records linked to North Atlantic Ocean circulation, *Clim. Dynam.*, accepted, doi:10.1007/s00382-016-3360-8, 2016.
- Eriksson, E.: Deuterium and oxygen-18 in precipitation and other natural waters Some theoretical considerations, *Tellus A*, **17**, 498–512, 1965.
- Field, R. D.: Observed and modeled controls on precipitation $\delta^{18}\text{O}$ over Europe: From local temperature to the Northern Annular Mode, *J. Geophys. Res.-Atmos.*, **115**, D12101, doi:10.1029/2009JD013370, 2010.
- Fischer, M. J.: Predictable components in global speleothem $\delta^{18}\text{O}$, *Quaternary Sci. Rev.*, **131**, 380–392, 2016.
- Fischer, M. J. and Baldini, L. M.: A climate-isotope regression model with seasonally-varying and time-integrated relationships, *Clim. Dynam.*, **37**, 2235–2251, 2011.
- Gat, J. R.: Oxygen and hydrogen isotopes in the hydrologic cycle, *Annu. Rev. Earth Planet. Sc.*, **24**, 225–262, 1996.
- Gulev, S. K., Zolina, O., and Grigoriev, S.: Extratropical cyclone variability in the Northern Hemisphere winter from the NCEP/NCAR reanalysis data, *Clim. Dynam.*, **17**, 795–809, 2001.
- Humer, G.: Niederschlagsisotopennetz Österreich, Daten, Wien, 04/1995 UBA-BE-033 Berichte, Band 033, ISBN: 3-85457-224-7, 110 pp., 1995.
- Hurrell, J. W.: Decadal Trends in the North-Atlantic Oscillation – Regional Temperatures and Precipitation, *Science*, **269**, 676–679, 1995.
- Hurrell, J. W. and VanLoon, H.: Decadal variations in climate associated with the north Atlantic oscillation, *Climatic Change*, **36**, 301–326, 1997.
- Hurrell, J. W., Kushnir, Y., Ottersen, G., and Visbeck, M.: The North Atlantic Oscillation: climatic significance and environmental impact, American Geophysical Union, 2003.
- Kaiser, A., Scheffinger, H., Kralik, M., Papesch, W., Rank, D., and Stichler, W.: Links between meteorological conditions and spatial/temporal variations in long-term isotope records from the Austrian precipitation network, *C&S PaperSeries*, **13**, 67–77, 2001.
- Kim, S.-T. and O’Neil, J. R.: Equilibrium and nonequilibrium oxygen isotope effects in synthetic carbonates, *Geochim. Cosmochim. Ac.*, **61**, 3461–3475, 1997.
- Langebroek, P. M., Werner, M., and Lohmann, G.: Climate information imprinted in oxygen-isotopic composition of precipitation in Europe, *Earth Planet. Sc. Lett.*, **311**, 144–154, doi:10.1016/j.epsl.2011.08.049, 2011.
- Lykoudis, S. P. and Argiriou, A. A.: Temporal trends in the stable isotope composition of precipitation: a comparison between the eastern Mediterranean and central Europe, *Theor. Appl. Climatol.*, **105**, 199–207, 2011.
- Mangini, A., Spötl, C., and Verdes, P.: Reconstruction of temperature in the Central Alps during the past 2000 yr from a $\delta^{18}\text{O}$ stalagmite record, *Earth Planet. Sc. Lett.*, **235**, 741–751, 2005.
- McDermott, F., Atkinson, T. C., Fairchild, I. J., Baldini, L. M., and Matthey, D. P.: A first evaluation of the spatial gradients in $\delta^{18}\text{O}$ recorded by European Holocene speleothems, *Global Planet. Change*, **79**, 275–287, 2011.
- Mischel, S. A., Scholz, D., and Spötl, C.: $\delta^{18}\text{O}$ values of cave drip water: a promising proxy for the reconstruction of the North Atlantic Oscillation?, *Clim. Dynam.*, **45**, 3035–3050, doi:10.1007/s00382-015-2521-5, 2015.
- Mook, W. G.: Introduction to isotope hydrology, Taylor & Francis, **8**, 2006.
- Mühlinghaus, C., Scholz, D., and Mangini, A.: Modelling fractionation of stable isotopes in stalagmites, *Geochim. Cosmochim. Ac.*, **73**, 7275–7289, 2009.

- Polag, D., Scholz, D., Mühlinghaus, C., Spötl, C., Schröder-Ritzrau, A., Segl, M., and Mangini, A.: Stable isotope fractionation in speleothems: Laboratory experiments, *Chem. Geol.*, 279, 31–39, 2010.
- Rayleigh, L.: LIX, On the distillation of binary mixtures, *The London, Edinburgh, and Dublin Philosophical Magazine and Journal of Science*, 4, 521–537, 1902.
- Rehfeld, K., Marwan, N., Breitenbach, S. F. M., and Kurths, J.: Late Holocene Asian summer monsoon dynamics from small but complex networks of paleoclimate data, *Clim. Dynam.*, 41, 3–19, 2013.
- Rozanski, K., Sonntag, C., and Münnich, K. O.: Factors controlling stable isotope composition of European precipitation, *Tellus*, 34, 142–150, 1982.
- Rozanski, K., Araguás-Araguás, L., and Gonfiantini, R.: Relation between long-term trends of oxygen-18 isotope composition of precipitation and climate, *Science*, 258, 981–985, 1992.
- Schürch, M., Kozel, R., Schotterer, U., and Tripet, J.-P.: Observation of isotopes in the water cycle—the Swiss National Network (NISOT), *Environ. Geol.*, 45, 1–11, 2003.
- Stumpp, C., Klaus, J., and Stichler, W.: Analysis of long-term stable isotopic composition in German precipitation, *J. Hydrol.*, 517, 351–361, 2014.
- Trenberth, K. E.: Atmospheric moisture residence times and cycling: Implications for rainfall rates and climate change, *Climatic Change*, 39, 667–694, 1998.
- Trigo, R. M., Osborn, T. J., and Corte-Real, J. M.: The North Atlantic Oscillation influence on Europe: climate impacts and associated physical mechanisms, *Clim. Res.*, 20, 9–17, 2002.
- Walczak, I. W., Baldini, J. U. L., Baldini, L. M., McDermott, F., Marsden, S., Standish, C. D., Richards, D. A., Andreo, B., and Slater, J.: Reconstructing high-resolution climate using CT scanning of unsectioned stalagmites: A case study identifying the mid-Holocene onset of the Mediterranean climate in southern Iberia, *Quaternary Sci. Rev.*, 127, 117–128, 2015.
- Wang, Y. H., Magnúsdóttir, G., Stern, H., Tian, X., and Yu, Y.: Decadal variability of the NAO: introducing an augmented NAO index, *Geophys. Res. Lett.*, 39, L21702, doi:10.1029/2012GL053413, 2012.
- Wassenburg, J. A., Dietrich, S., Fietzke, J., Fohlmeister, J., Jochum, K. P., Scholz, D., Richter, D. K., Sabaoui, A., Spötl, C., Lohmann, G., Andreae, M. O., and Immenhauser, A.: Reorganization of the North Atlantic Oscillation during early Holocene deglaciation, *Nat. Geosci.*, 9, 602, doi:10.1038/NGEO2767, 2016.
- Werner, M., Langebroek, P. M., Carlsen, T., Herold, M., and Lohmann, G.: Stable water isotopes in the ECHAM5 general circulation model: Toward high-resolution isotope modeling on a global scale, *J. Geophys. Res.*, 116, D15109, doi:10.1029/2011JD015681, 2011.
- Wiedner, E., Scholz, D., Mangini, A., Polag, D., Mühlinghaus, C., and Segl, M.: Investigation of the stable isotope fractionation in speleothems with laboratory experiments, *Quatern. Int.*, 187, 15–24, 2008.